Phenothiazine Inhibits Neuroinflammation and Inflammasome Activation Independent of Hypothermia After Ischemic Stroke

Sichao Guo
Beijing Luhe Hospital
Xiaokun Geng
Beijing Luhe Hospital
Hangil Lee
Wayne State University
Yuchuan Ding (yding@med.wayne.edu)
Wayne State University School of Medicine https://orcid.org/0000-0001-5358-1660

Research Article

Keywords: Ischemic Stroke, chlorpromazine and promethazine (C+P), JAK2/STAT3, p38, HIF-1α, FoxO1

Posted Date: July 7th, 2021

DOI: https://doi.org/10.21203/rs.3.rs-673718/v1

Version of Record: A version of this preprint was published at Molecular Neurobiology on August 29th, 2021. See the published version at https://doi.org/10.1007/s12035-021-02542-3.

Abstract

A depressive or hibernation-like effect of chlorpromazine and promethazine (C + P) on brain activity was reported to induce neuroprotection, with or without induced-hypothermia. However, the underlying mechanisms remain unclear. The current study evaluated the pharmacological function of C + P on the inhibition of neuroinflammatory response and inflammasome activation after ischemia/reperfusion. A total of 72 adult male Sprague-Dawley rats were subjected to 2 h middle cerebral artery occlusion (MCAO) followed by 6 or 24 h reperfusion. At the onset of reperfusion, rats received C + P (8 mg/kg) with temperature control. Brain cell death was detected by measuring CD68 and myeloperoxidase (MPO) levels. Inflammasome activation was measured by mRNA levels of NLRP3, IL-1β, and TXNIP, and protein quantities of NLRP3, IL-1β, TXNIP, cleaved-Caspase-1, and IL-18. Activation of JAK2/STAT3 pathway was detected by the phosphorylation of STAT3 (p-STAT3) and JAK2 (p-JAK2), and the co-localization of p-STAT3 and NLRP3. Activation of the p38 pathway was assessed with the protein levels of p-p38/p38. The mRNA and protein levels of HIF-1α, FoxO1, and p-FoxO1, and the co-localization of p-STAT3 with HIF-1α or FoxO1 were quantitated. As expected, C + P significantly reduced cell death and attenuated the neuroinflammatory response as determined by reduced CD68 and MPO. C + P decreased ischemia-induced inflammasome activation, shown by reduced mRNA and protein expressions of NLRP3, IL-1β, TXNIP, cleaved-Caspase-1, and IL-18. Phosphorylation of JAK2/STAT3 and p38 pathways and the co-localization of p-STAT3 with NLRP3 were also inhibited by C + P. Furthermore, mRNA levels of HIF-1α and FoxO1 were decreased in the C + P group. While C + P inhibited HIF-1α protein expression, it increased FoxO1 phosphorylation, which promoted the exclusion of FoxO1 from the nucleus and inhibited FoxO1 activity. At the same time, C + P reduced the co-localization of p-STAT3 with HIF-1α or FoxO1. In conclusion, C + P treatment conferred neuroprotection in stroke by suppressing neuroinflammation and NLRP3 inflammasome activation. The present study suggests that JAK2/STAT3/p38/HIF-1α/FoxO1 are vital regulators and potential targets for efficacious therapy following ischemic stroke.

Introduction

Acute ischemic stroke causes irreversible cell damage, leading to severe mortality and morbidity worldwide [1–3]. Current clinical treatments are limited to reperfusion strategies with tissue plasminogen activator (tPA) or thrombectomy, which are only applied and beneficial to a small proportion of stroke victims because of the limited therapeutic time window [4].

Chlorpromazine and promethazine (C + P), both members of the phenothiazine class of neuroleptic drugs, have been widely used for their antipsychotic and sedative effects [5, 6]. Moreover, phenothiazine drugs have been demonstrated to induce neuroprotection in ischemia [6]. A robust neuroprotective effect was identified with C + P combination therapy in severe transient and permanent ischemic stroke [6, 7]. The neuroprotective role may partially depend on the hypothermia induced by C + P [6, 8, 9]. In order to comprehensively understand the pharmacological effects of C + P therapy, the mechanisms underlying its neuroprotective effects without hypothermia induction remain to be determined.

The increased neuroinflammatory response and inflammasome activation act as key components in the pathogenesis of ischemic stroke. After stroke, the interruption and reperfusion of blood flow in brain tissue trigger the infiltration of inflammatory cells and cause a robust inflammatory response, thereby inducing neuronal apoptosis and death [10]. Neuroprotection with C + P has been identified to be related with inhibition of the inflammatory response and NLRP3 inflammasome activation after ischemic stroke [11, 12]. The NOD-like receptor family pyrin domain containing 3 (NLRP3) inflammasome is one of the best characterized of the nucleotide-binding oligomerization domain (NOD)-like receptors (NLR) family [13–15]. Upregulation of the NLRP3 inflammasome results in the cleavage of pro-caspase-1. Consequently, caspase-1 is activated, which leads to the promotion of interleukin-1β (IL-1β) and interleukin-18 (IL-18) maturation and activation of pyroptosis, which is a type of inflammatory cell death [16, 17]. It has been reported that the NLRP3 inflammasome activation was a vital mediator of inflammatory responses after ischemic stroke [18]. Janus kinase 2 (JAK2)/signal transducer and activator of transcription 3 (STAT3) is a classic pathway that promotes inflammation [19]. It is related to pyroptosis and is highly activated after ischemic stroke [20, 21]. p38 is activated after cerebral ischemia and induces a series of pathological processes such as inflammation and NLRP3 inflammasome activation [22–24]. Hypoxia-inducible factor 1 alpha (HIF-1 alpha) and Forkhead box transcription factor O1 (FoxO1) are also related to the inflammatory response and inflammasome activation[25, 18, 26]. Therefore, the current study further investigated the pharmacological function of C + P on the inhibition of neuroinflammatory response and inflammasome activation after ischemia/reperfusion through JAK2/STAT3/p38/HIF-1α/FoxO1 regulation.

Experimental Procedures

Subjects

A total of 72 adult male Sprague-Dawley rats (280–300 g, Vital River Laboratory Animal Technology Co., Ltd., Beijing, China) were used in this study, which adhered to the guidelines set forth by the Institutional Animal Investigation Committee of the Capital Medical University. The rats were housed and maintained under a 12 h light/dark cycle in the same animal care facility for the entire duration of the study. All efforts were made to minimize any suffering and reduce the total number of animals used in the study. Animals were randomly divided into the following groups: (1) a sham-operated group without MCAO for RNA/protein assay (n = 7) and immunofluorescence staining (n = 6); (2) 2 h MCAO followed by 6 or 24 h of reperfusion for RNA/protein assay (n = 7x2), at 24 h for immunofluorescence staining (n = 6), and at 48 h for TTC assay (n = 7); (3) 2 h MCAO and C + P with temperature control at 37^0C followed by 6 or 24 h of reperfusion for RNA/protein assay (n = 7x2), at 24 h for immunofluorescence staining (n = 6), and at 48 h for TTC assay (n = 7). Rats (n = 5, less than 10%) were excluded for further analysis because of death, brain hemorrhage, or lack of ischemic injury based on neurological deficits and confirmed with 2,3,5-triphenyltetrazolium chloride (TTC) staining. All procedures and data analysis were carried out blindly and randomly [27]. In all temperature-controlled groups, rats were placed on 37^0C insulation blankets and under a warm ambient light source to maintain their body temperatures.

Focal Cerebral Ischemia

The model used in this study has been described previously by us [28]. Briefly, rats were anesthetized in a chamber with 1–3% isoflurane and a mixture of 70% nitrous oxide and 30% oxygen. Throughout the surgical procedure, the anesthesia was maintained with a face mask using 1% isoflurane delivered from a calibrated precision vaporizer. To reduce inter-animal variability, poly-L-lysine-coated intraluminal nylon (4.0) sutures were used to occlude the MCA thus yielding consistently sized infarct.

Administration of Chlorpromazine and Promethazine (C + P)

The combination of C + P (1:1) at doses of 8 mg/kg in saline was injected intraperitoneally (IP) at the onset of reperfusion in ischemic rats as determined previously by us [6]. Then, a second injection with one-third of the original dose was added 2 h later to enhance the drugs' therapeutic effects.

Infarct Volume Measurement

After 48 h of reperfusion, the brains were resected from ischemic rats and cut into 2-mm-thick slices (brain matrix) and treated with 2,3,5-triphenyltetrazolium chloride (TTC; Sigma-Aldrich, St. Louis, MO, USA) for staining. The infarct volume was calculated using an indirect method to ensure that the error attributable to edema was reduced as much as possible. Briefly, the infarct cross-sectional area in each brain slice was calculated using Image J. The infarct volume of each brain slice was calculated as the difference between the total volume of the left hemisphere and the volume of the non-infarcted right hemisphere, divided by the total volume of the left hemisphere [6].

Real-time qRT-PCR

Brain tissue samples containing the frontoparietal cortex and striatum, which are MCA-supplied territories, were processed as previously described by us [11]. The Trizol reagent (Invitrogen, USA) was used to extract total RNA according to manufacturer directions. Subsequently, RNA was reverse transcribed into cDNA with the High Capacity cDNA Reverse Transcription kit (Applied Biosystems, USA). Quantitative PCR was conducted using the SYBR Green PCR Master Mix (Applied Biosystems, USA) on the ABI PRISM 7500 real-time cycler (Applied Biosystems). Primer sequences for IL-1β, NLRP3, thioredoxin-interacting protein (TXNIP), HIF-1α, FoxO1 and β-actin are displayed in Table 1.

Table 1
Primers used for RT-qPCR analysis.

Genes	Primer sequence (5′-3′) forward	Primer sequence (5′-3′) reverse
IL-1β	TCCAGGATGAGGACCCAAGC	TCGTCATCATCCCACGAGTCA
NLRP3	AGTGGATAGGTTTGCTGGG	TGGGTGTAGCGTCTGTTGAG
TXNIP	AGGTGAGAACGAGATGGTA	CTCTTGAGTTGGCTGGCTG
FoxO1	CAGCCAGGCACCTCATAACA	TCAAGCGGTTCATGGCAGAT
HIF-1α	TCAAGTCAGCAACGTGGAAG	TATCGAGGCTGCGTCGACTG
β-actin	CAAGAAGGTGGTGAAGCAG	AAAGGTGGAAGAATGGGAG

Enzyme-linked Immunosorbent Assay (ELISA)

Tissue samples from the ischemic hemispheres were processed as previously described by us [18]. According to the manufacturer's instructions, 500 μl of extraction lysis buffer was added to the tube for every 10 mg of infarcted tissue, which was mixed with an electric homogenizer. ELISA kits were used to measure IL-18 (ml002816, Shanghai Enzyme-linked Biotechnology Co, China), IL-1β (ml037361, Shanghai Enzyme-linked Biotechnology Co, China), CD68 (ml059367, Shanghai Enzyme-linked Biotechnology Co, China), MPO (ml003250, Shanghai Enzymelinked Biotechnology Co, China) and cell death from apoptosis (m1059429, Shanghai Enzymelinked Biotechnology Co, China).

TUNEL Assay

The TUNEL assay was used to investigate DNA fragmentation, which was performed with a commercial kit (In situ Cell Death Detection Kit, Fluoresce, Roche, Indianapolis, IN, USA) as outlined in our previous research [18]. Images were acquired from the infarcted cortex of the brain sections. In accordance with the manufacturer's instructions, the fixed and permeabilized slides were incubated in 50 μl of the TUNEL reaction mixture at 37℃ for 1 h. The positive TUNEL staining was visualized using a fluorescence microscope (DM4000, Leica, Germany). The infarcted cortex was acquired randomly from different positions and images per section. The $TUNEL^+$ cells were counted using the manual cell counting tool in Image J. In a blind manner, the values of all sections from each group were acquired and used for subsequent statistical analysis. The percentage of apoptotic cells was calculated as the percentage of $TUNEL^+$ cells over total cells. The percentage of positively staining cells was used to determine cell death with the TUNEL index.

Immunofluorescence Staining

Immunofluorescence staining was used to detect the expression of p-STAT3, NLRP3, FoxO1 and HIF-1α as described previously by us [8]. Images acquired from the infarcted cortex of the brain sections were measured. For immunofluorescence, sections were incubated with primary p-STAT3(Cell Signaling Technology, 9145S, 4113S), NLRP3(Novus Biologicals, NBP2-12446), FoxO1(Cell Signaling Technology,

14952S), and HIF-1α (Novus Biologicals, NB100-105) antibodies overnight at 4°C, followed by application of fluorescence conjugated secondary antibodies (Alexa Fluor 594 for FoxO1, HIF-1α, 1:500, ThermoFisher, A-11005; Alexa Fluor 488 for p-STAT3, 1:500, ThermoFisher, A-11008; Alexa Fluor 594 for NLRP3, 1:500, ThermoFisher, A-11012; Alexa Fluor 488 for p-STAT3, 1:500, ThermoFisher, A-11001) at room temperature for 1 h. An antifade mounting medium with DAPI (Zhongshan Biotechnology) was used to mount the slides. The images were examined with a fluorescence microscope (DM4000, Leica, Germany). After blinding the groups, p-STAT3$^+$, NLRP3$^+$, FoxO1$^+$ and HIF-1α$^+$ cells were counted using the Image J manual cell counting tool. The values were averaged by groups and used for statistical analysis. The percentage of p-STAT3$^+$/ NLRP3$^+$/ FoxO1$^+$ /HIF-1α$^+$ cells was calculated as the percentage of positively staining cells over total cells. The percentage of co-localizing cells was calculated as the percentage of co-localizing cells over total cells.

Protein Expression

Western blot analysis was used to detect protein expression in brain tissue and cells, as described previously by us [29]. Tissue from the right cerebral hemisphere, consisting of the frontoparietal cortex and striatum, were processed as tissue samples for further analysis. Tissues and cells were lysed with the Mammalian Protein Extraction Reagent (Thermo Scientific). Proteins extracted from rat brain and cell isolates were loaded onto gels for electrophoresis. Proteins were transferred to a polyvinylidene fluoride membrane. Membranes were incubated with a primary antibody (1:1,000, rabbit anti-IL-1β antibody, Abcam, ab9722; 1:1,000, rabbit anti-TXNIP antibody, Cell Signaling Technology, 14715S; 1:1,000, rabbit anti-Caspase-1 antibody, Santa Cruz, sc-56036; 1:1,000, rabbit anti-p38 antibody, Cell Signaling Technology, 9212S; 1:1,000, rabbit anti-p-p38 antibody, Cell Signaling Technology, 9211S; 1:1,000, rabbit anti-JAK2, Cell Signaling Technology, 3230S; 1:1,000, rabbit anti-p-JAK2, Cell Signaling Technology, 3776S; 1:1,000, rabbit anti-STAT3, Cell Signaling Technology, 4904S; 1:1,000, rabbit anti-p-STAT3, Cell Signaling Technology, 9145S; 1:1,000, rabbit anti-NLRP3, Novus Biologicals, NBP2-12446; 1:1,000, rabbit anti-p-FoxO1, Cell Signaling Technology, 84192S; 1:1,000, rabbit anti-FoxO1, Novus Biologicals, NB-1002312; 1:1,000, rabbit anti-HIF-1α, Novus Biologicals, NB100-105; 1:2,000, β-actin, Santa Cruz) for 16 h at 4ºC. Next, membranes were incubated with a secondary antibody (goat anti-rabbit IgG, Cell Signaling Technology) for 2 h at room temperature. An enhanced chemiluminescence system was used to detect immunoreactive bands. Western blot images for each antibody were analyzed using an image analysis program (Image J, v.1.44, National Institutes of Health, USA) to quantify protein expression in terms of relative image density.

Statistical Analysis

Statistical analyses were performed with Graphpad Prism v8.0 (Graphpad Software, San Diego, CA, USA). The differences among groups were calculated using one-way ANOVA with the significance level set at $p < 0.05$. Post hoc comparisons between groups were conducted using the least significant difference (LSD) method. All data and values were expressed as mean ± SE.

Results

C + P Treatment Reduced Brain Injury after Stroke

Infarct volume after stroke as determined by TTC staining was significantly decreased by C + P with temperature control treatment when compared to the stroke group at 48 h after reperfusion ($p < 0.01$, Fig. 1A). When compared to the sham group, apoptotic cell death, measured by ELISA, was also significantly increased after MCAO, but the administration of C + P with temperature control decreased cell death levels at 6 and 24 h after reperfusion ($p < 0.05$, Fig. 1B). In addition, apoptotic cell death in ischemia/reperfusion group as determined by the TUNEL assay was largely increased when compared to the sham group at 24 h after reperfusion ($p < 0.001$, Fig. 1C). Remarkably, apoptosis was significantly diminished by treatment with C + P at 37^0C.

C + P Treatment Attenuated the Neuroinflammatory Response

Compared to the sham group, the levels of MPO (a neutrophil marker) and CD68 (a macrophage marker) measured by ELISA were increased after stroke at 6 and 24 h reperfusion ($p < 0.001$). Meanwhile, C + P significantly reduced the levels of MPO and CD68 (Fig. 2A&B).

C + P Treatment Decreased NLRP3 Inflammasome Activation

C + P significantly ameliorated the remarkable elevation of IL-1β levels at 6 and 24 h of reperfusion as well as IL-18 levels at 24 h of reperfusion, as detected by ELISA (Fig. 3A&B). qRT-PCR showed increased mRNA quantities of IL-1β and NLRP3 after MCAO ($p < 0.01$, $p < 0.001$), which were significantly reduced by C + P therapy at 6 and 24 h reperfusion. Similarly, mRNA levels of TXNIP were increased after ischemia/reperfusion ($p < 0.05$), but C + P ($p < 0.001$) reduced them at 24 h of reperfusion (Fig. 4A, B, C). Western blot showed that ischemic rats exposed to 2 h MCAO observed significant increase in the IL-1β protein levels at 6 and 24 h reperfusion. The overexpression was significantly reversed by C + P treatment (Fig. 5A). At 6 and 24 h of reperfusion, NLRP3 protein levels were increased ($p < 0.05$). Remarkably, C + P significantly reduced NLRP3 levels at 6 and 24 h of reperfusion ($p < 0.001$, Fig. 5B). Similarly, $NLRP3^+$ cells were detected by immunofluorescence at 24 h of reperfusion. As expected, C + P administration markedly reduced the elevation of NLRP3 induced by MCAO ($p < 0.001$, Fig. 7A&C). Expression of TXNIP protein was significantly increased at 24 h of reperfusion, while C + P decreased TXNIP synthesis ($p < 0.001$, Fig. 5C). There was a significant increase of cleaved-Caspase 1 at 6 and 24 h of reperfusion, but C + P treatment at 37^0C reduced its levels ($p < 0.05$, Fig. 5D).

C + P Decreased Activation of JAK2/STAT3 And P38 Pathways after Ischemia

Western blot showed MCAO significantly increased the phosphorylation of p38 at 6 h and 24 h of reperfusion ($p < 0.05$) and JAK2 at 6 h of reperfusion ($p < 0.05$). C + P treatment significantly decreased the phosphorylation of p38 and JAK2. Similar results were obtained when the ratios of phosphorylated proteins to total protein were calculated. An increase in the ratios of p-p38/p38 at 6 and 24 h of reperfusion ($p < 0.05$, $p < 0.01$) and p-JAK2/JAK2 at 6 h of reperfusion ($p < 0.05$) were seen after stroke, which were significantly suppressed by C + P (Fig. 6A, B, C). MCAO also elicited increases in the phosphorylation levels of STAT3 and the ratio of p-STAT3/STAT3 at 6 h and 24 h of reperfusion as detected by Western blot ($p < 0.001$, Fig. 6A&D), as well as at 24 h of reperfusion as measured by immunofluorescence assay (Fig. 7A&B). Again, rats treated with C + P after MCAO significantly attenuated the effects. In order to further assess the relationship between p-STAT3 and NLRP3, the cellular co-localization of p-STAT3 and NLRP3 was examined. Immunofluorescence demonstrated that p-STAT3 was present in $NLRP3^+$ cells at 24 h reperfusion. After C + P administration, the number of brain p-$STAT3^+$/ $NLRP3^+$ cells were reduced ($p < 0.001$, Fig. 7A&D).

C + P Treatment Decreased Expression Of HIF-1α and FoxO1 Induced by Ischemia

Compared to the sham group, mRNA levels of HIF-1α ($p < 0.001$) and FoxO1 ($p < 0.05$) increased in the stroke group after 6 h reperfusion, but were significantly reduced by C + P treatment at 6 h reperfusion (Fig. 8A&B).

Western blot results showed that MCAO increased expressions of HIF-1α at 6 and 24 h reperfusion ($p < 0.001$, $p < 0.05$). C + P treatment significantly reduced the expression of HIF-1α at 6 and 24 h reperfusion ($p < 0.001$, $p < 0.01$, Fig. 9A). Immunofluorescence assay showed similar results, where C + P treatment attenuated $HIF\text{-}1\alpha^+$ cells at 24 h reperfusion ($p < 0.001$, Fig. 10A&B). To explore the relationship between p-STAT3 and HIF-1α, the cellular co-localization of p-STAT3 and HIF-1α was detected using immunofluorescence at 24 h reperfusion. The number of brain p-$STAT3^+$/ $HIF\text{-}1\alpha^+$ cells were decreased after C + P administration ($p < 0.001$ Fig. 10A&C).

Phosphorylation levels of FoxO1 was decreased after MCAO at 6 h of reperfusion ($p < 0.05$), while C + P reversed the reduced level of p-FoxO1 ($p < 0.01$). In contrast, brain FoxO1 was significantly increased at 24 h of reperfusion. The use of C + P at 6 h and 24 h reperfusion decreased FoxO1 expressions ($p < 0.05$, $p < 0.001$). Furthermore, the ratio of p-FoxO1/FoxO1 significantly decreased after MCAO ($p < 0.05$) but increased with C + P at 6 and 24 h reperfusion ($p < 0.001$, Fig. 9B), suggesting entering of FoxO1 into the nucleus and activation of FoxO1 caused by ischemia was inhibited by C + P treatment. Compared with the sham group, the number of FoxO1 positive cells in the brain tissue of the MCAO group was significantly increased ($p < 0.001$). C + P treatment reduced the number of $FoxO1^+$ cells in ischemic brain tissues in rats at 24 h of reperfusion ($p < 0.001$, Fig. 11A&B). The co-localization of p-STAT3 and FoxO1 was detected by immunofluorescence at 24 h of reperfusion. Similar to the expression of HIF-1α, the number of p-$STAT3^+$/ $FoxO1^+$ cells were inhibited by C + P administration ($p < 0.001$, Fig. 11A&C). These

results suggest that C + P inhibition of inflammasome activation through p-STAT3 may be related to its effects on FoxO1.

Discussion

In the present study, we elucidated that C + P with temperature control reduced brain damage after stroke. This may be due to its attenuation of the neuroinflammatory response and inflammasome activation following ischemic stroke, shown by reduced CD68 and MPO and attenuated expressions of NLRP3, IL-1β, TXNIP, cleaved-Caspase-1, and IL-18. The phosphorylation activation of JAK2/STAT3 and p38 pathways and co-localization of p-STAT3 with NLRP3 were also inhibited by C + P. Furthermore, C + P reduced the expression of HIF-1α protein and decreased the activity of FoxO1 through promoting its nuclear release and inhibiting its activation. At the same time, C + P reduced the co-localization of p-STAT3 with HIF-1α and p-STAT3 with FoxO1. Taken together, these results suggest C + P repressed JAK2/STAT3 and p38 signaling pathways as well as FoxO1 and HIF-1α in a hypothermia-independent manner, leading to reduced neuroinflammatory response and inflammasome activation, which ultimately attenuated brain damage.

In our previous study, we found that the administration of the classic neuroleptic phenothiazines, C + P, conferred neuroprotection in models of severe stroke by suppressing the damaging cascade of metabolic events, which was partially dependent on drug induced hypothermia [6, 30]. Chlorpromazine, a phenothiazine, was shown to suppress the production of proinflammatory cytokines including TNF-α, IL-1β, and IL-6 [31–33]. Moreover, the neuroprotective role of C + P in ischemic stroke seemed to be dependent on its amelioration of hyperglycolysis [8], blood–brain barrier disruption [28], inflammation [11], inflammasome activation [12], and apoptosis [34]. C + P can induce hypothermia, but its neuroprotective effect post-ischemic stroke was partially independent of its hypothermic effect [6, 8, 11, 12]. In the present study, we verified how C + P exerted pharmacological and neuroprotective effects without hypothermia, namely, the inhibitory effects of C + P on the inflammatory response and inflammasome activation [11, 12].

Macrophages and neutrophils participate in brain inflammation after ischemic stroke and high levels of these cells are associated with poor prognosis [35]. Myeloperoxidase (MPO) is a heme containing peroxidase that is expressed in the aforementioned inflammatory cells [36]. MPO has been observed to be elevated in the context of ischemic strokes, in both animal and clinical studies [37, 38]. CD68 is an inflammatory marker specific to activated microglia that is usually not expressed in surveillant microglia [39, 40]. It is also associated with age dependent neuroinflammation [41]. In the context of ischemic stroke, MPO and CD68 were representative of apoptotic cell death [42] and were attenuated by HIF-1α inhibition[18], indicating that they serve as accurate markers of inflammation. In the present study, C + P reduced MPO and CD68 levels, which represented suppression of inflammation through inhibition of immune cell infiltration and apoptotic cell death.

C + P repressed the MCAO induced increases of NLRP3, IL-1β, IL18, TXNIP, and cleaved-Caspase 1, resulting in the inhibition of inflammasome activation. NLRP3 is an indispensable inflammasome of the NLR family and is activated under ischemic conditions. In addition, its levels are related to increased infarction and apoptotic cell death that accompanies ischemic injury [18]. The up-regulation of caspase-1 activated by NLRP3 inflammasome promotes the maturation of IL-1β and IL-18, which are pyrogens involved in inflammatory apoptosis [17]. During the cerebral ischemia reperfusion injury, TXNIP dissociates from the Trx1/TXNIP complex and enters the cytoplasm to activate the NLRP3 inflammasome [43].

Chlorpromazine has been reported to decrease the phosphorylation of STAT3 [44]. Treatment with chlorpromazine may induce the expression of distinct genes against apoptosis progression via the JAK-STAT signaling pathway [45]. JAK/STAT signaling pathway is important for the progression of neurological diseases including stroke, traumatic brain injury, brain tumors, and neurodegenerative diseases [46, 47]. Many evidences have indicated that the JAK2/STAT3 signaling is phosphorylation activated during cerebral ischemia and mediates oxidative stress, inflammatory response, and neuronal apoptosis [46, 20, 19]. In both MCAO and OGD experimental models, the expression of p-STAT3 increased, which resulted in the activation of inflammasomes [48]. It has been reported that the expression of p-STAT3 was co-localized with NLRP3-positive cells and upregulated NLRP3 via STAT3-dependent histone acetylation [49]. p38 mitogen-activated protein kinase (MAPK) activity is involved in the inflammatory response during stroke, as supported by the observation that p-p38 expression is upregulated in the ischemia area [23, 50]. p38 MAPK signaling pathway induced the activation of the NLRP3 inflammasome and macrophage pyroptosis [51]. Consistent with previous findings, we found that the activation of JAK2/ STAT3 and p38 and the co-localization of p-STAT3 with NLRP3 were significantly increased following postischemia, but attenuated by C + P therapy.

When cells are exposed to hypoxia, there is an increase in hypoxia-induced factor-1α (HIF-1α) expression [52]. There is also an elevated expression of HIF-1α during periods of ischemia/reperfusion in neurons [25]. HIF-1α mediates inflammatory response after cerebral ischemia/reperfusion injury [25]. Moreover, our previous study reported that HIF-1α mediated NLRP3 inflammasome dependent pyroptotis following ischemic stroke [18]. The activation of p38 through phosphorylation stabilizes HIF-1α, which in turn may be involved in the increased production of IL-1β [53]. Phosphorylated STAT3 stimulates and binds to HIF-1α, promoting its stability during hypoxia [54]. Mammalian FoxO proteins are assigned to the O class of the forkhead box class transcription factors [55]. It has been reported that the expression of FoxO1 increased after ischemia/reperfusion [56, 57]. Additionally, after stroke, the phosphorylation of FoxO1, which represents its inactive form, was decreased, underwent nuclear translocation, and activated its target genes including inflammation pathways [26]. Activated p38 mediates the translocation of FoxO1 into the nucleus and the binding of FoxO1 to the promoter of TXNIP, promoting the upregulation of the TXNIP protein and further increasing inflammasome activation [58–61]. FoxO1 can act as a coactivator of STAT3, correlating with the physical association of their co-localization in the nuclear regions [62]. Moreover, HIF-1α drives FoxO1 expression by binding directly to the hypoxia-responsive elements within its promoter region [63, 64]. In the present study, we found that C + P suppressed the expression of HIF-1α

after exposure to ischemic stroke. C + P also repressed the activation of FoxO1 through the inhibition of FoxO1 and increasing the phosphorylation thereof, leading to its exclusion from the nucleus. Moreover, we confirmed that MCAO induced the co-localization of p-STAT3 with HIF-1α or FoxO1, but C + P significantly reduced this trend. In summary, we observed that C + P induced pharmacological neuroprotection through inhibition of the NLRP3 inflammasome expression, which is mediated by HIF-1α and FoxO1 and may be related to the JAK2/STAT3 and p38 pathway.

In conclusion, the results of the present study indicated that C + P treatment conferred neuroprotection and rescued brain tissue after ischemia/reperfusion by suppressing neuroinflammatory responses and NLRP3 inflammasome activation in the absence of hypothermia induction. These therapeutic effects are associated with alterations of the JAK2/STAT3 and p38 pathways and subsequent inactivation of HIF-1α and FoxO1. The present study suggests that the JAK2/STAT3/p38/HIF-1α/FoxO1 pathway is a key regulator of ischemic stroke, and hence a potential therapeutic target.

Declarations

AcknowledgementsNot applicable

Funding

This work was supported in part by the National Natural Science Foundation of China (81871838, 82001277), the Beijing Tongzhou District Financial Fund, the Science and Technology Plan of Beijing Tongzhou District (KJ2020CX002), the Laboratory Development Funds of Luhe Hospital (2021).

Availability of data and material

All data generated or analyzed during this study are included in this published article.

Code availability

Not applicable

Authors' contributions

Conceptualization: Yuchuan Ding, Xiaokun Geng and Sichao Guo.; Methodology: Sichao Guo; Formal analysis and investigation: Sichao Guo; Writing - original draft preparation: Sichao Guo; Writing - review and editing: Yuchuan Ding, Xiaokun Geng and Hangil Lee; Funding acquisition: Xiaokun Geng; Resources: Yuchuan Ding and Xiaokun Geng; Supervision: Yuchuan Ding and Xiaokun Geng.

Ethics Approval

Animal experiments were approved by the Institutional Animal Investigation Committee of the Capital Medical University and were performed in accordance with the Guidelines for Animal Experiments at Capital Medical University.

Consent to Participate No human subjects were involved in this research, so consent to participate is not relevant.

Consent for Publication All authors have approved this manuscript and consented to its submission for publication.

Conflict of Interest The authors declare no competing interests

References

1. Phipps MS, Cronin CA (2020) Management of acute ischemic stroke. BMJ 368:l6983. doi:10.1136/bmj.l6983
2. Ren C, Li N, Gao C, Zhang W, Yang Y, Li S, Ji X, Ding Y (2020) Ligustilide provides neuroprotection by promoting angiogenesis after cerebral ischemia. Neurological research 42(8):683–692. doi:10.1080/01616412.2020.1782122
3. Fan X, Elkin K, Shi Y, Zhang Z, Cheng Y, Gu J, Liang J, Wang C, Ji X (2020) Schisandrin B improves cerebral ischemia and reduces reperfusion injury in rats through TLR4/NF-κB signaling pathway inhibition. Neurological research 42(8):693–702. doi:10.1080/01616412.2020.1782079
4. González-Nieto D, Fernández-Serra R, Pérez-Rigueiro J, Panetsos F, Martinez-Murillo R, Guinea GV (2020) Biomaterials to Neuroprotect the Stroke Brain: A Large Opportunity for Narrow Time Windows. Cells 9 (5). doi:10.3390/cells9051074
5. Cotã© CJ, Karl HW, Notterman DA, Weinberg JA, Mccloskey C (2000) Adverse sedation events in pediatrics: analysis of medications used for sedation. Pediatrics 106(4):633–644
6. Geng X, Li F, Yip J, Peng C, Ding Y (2017) Neuroprotection by Chlorpromazine and Promethazine in Severe Transient and Permanent Ischemic Stroke. Mol Neurobiol 54(10):8140–8150
7. Liu S, Geng X, Forreider B, Xiao Y, Kong Q, Ding Y, Ji X (2015) Enhanced beneficial effects of mild hypothermia by phenothiazine drugs in stroke therapy. Neurological research 37(5):454–460
8. Guo S, Cosky E, Li F, Guan L, Ji Y, Wei W, Peng C, Geng X, Ding Y (2021) An inhibitory and beneficial effect of chlorpromazine and promethazine (C + P) on hyperglycolysis through HIF-1α regulation in ischemic stroke. Brain research 1763:147463. doi:10.1016/j.brainres.2021.147463
9. Kuczynski AM, Demchuk AM, Almekhlafi MA (2019) Therapeutic hypothermia: Applications in adults with acute ischemic stroke. Brain circulation 5(2):43–54. doi:10.4103/bc.bc_5_19
10. Wang J, Mao J, Wang R, Li S, Wu B, Yuan Y (2020) Kaempferol Protects Against Cerebral Ischemia Reperfusion Injury Through Intervening Oxidative and Inflammatory Stress Induced Apoptosis. Front Pharmacol 11:424–424. doi:10.3389/fphar.2020.00424
11. Guan LGS, Yip J, Elkin KB, Li F, Peng C, Geng X, Ding Y (2019) Artificial Hibernation by Phenothiazines: A Potential Neuroprotective Therapy Against Cerebral Inflammation in Stroke. Curr Neurovasc Res 16(3):232–240

12. Jiang Q, Wills M, Geng X, Ding Y (2021) Chlorpromazine and promethazine reduces Brain injury through RIP1-RIP3 regulated activation of NLRP3 inflammasome following ischemic stroke. Neurological research:1–9. doi:10.1080/01616412.2021.1910904
13. Donovan C, Liu G, Shen S, Marshall JE, Kim RY, Alemao CA, Budden KF, Choi JP, Kohonen-Corish M, El-Omar EM, Yang IA, Hansbro PM (2020) The role of the microbiome and the NLRP3 inflammasome in the gut and lung. J Leukoc Biol 108(3):925–935. doi:10.1002/jlb.3mr0720-472rr
14. An S, Hu H, Li Y, Hu Y (2020) Pyroptosis Plays a Role in Osteoarthritis. Aging Dis 11(5):1146–1157. doi:10.14336/AD.2019.1127
15. Wu J, Lin S, Wan B, Velani B, Zhu Y (2019) Pyroptosis in Liver Disease: New Insights into Disease Mechanisms. Aging Dis 10(5):1094–1108. doi:10.14336/AD.2019.0116
16. Davis BK, Wen H, Ting JP (2011) The inflammasome NLRs in immunity, inflammation, and associated diseases. Annu Rev Immunol 29:707–735. doi:10.1146/annurev-immunol-031210-101405
17. Rathinam VA, Fitzgerald KA (2016) Inflammasome Complexes: Emerging Mechanisms and Effector Functions. Cell 165(4):792–800. doi:10.1016/j.cell.2016.03.046
18. Jiang Q, Geng X, Warren J, Eugene Paul Cosky E, Kaura S, Stone C, Li F, Ding Y (2020) Hypoxia Inducible Factor-1α (HIF-1α) Mediates NLRP3 Inflammasome-Dependent-Pyroptotic and Apoptotic Cell Death Following Ischemic Stroke. Neuroscience 448:126–139. doi:10.1016/j.neuroscience.2020.09.036
19. Dong Y, Hu C, Huang C, Gao J, Niu W, Wang D, Wang Y, Niu C (2021) Interleukin-22 Plays a Protective Role by Regulating the JAK2-STAT3 Pathway to Improve Inflammation, Oxidative Stress, and Neuronal Apoptosis following Cerebral Ischemia-Reperfusion Injury. Mediators Inflamm 2021:6621296. doi:10.1155/2021/6621296
20. Liang Z, Wu G, Fan C, Xu J, Jiang S, Yan X, Di S, Ma Z, Hu W, Yang Y (2016) The emerging role of signal transducer and activator of transcription 3 in cerebral ischemic and hemorrhagic stroke. Progress in neurobiology 137:1–16. doi:10.1016/j.pneurobio.2015.11.001
21. Chang L, Niu F, Chen J, Cao X, Liu Z, Bao X, Xu Y (2019) Ghrelin improves muscle function in dystrophin-deficient mdx mice by inhibiting NLRP3 inflammasome activation. Life sciences 232:116654. doi:10.1016/j.lfs.2019.116654
22. Guo RB, Wang GF, Zhao AP, Gu J, Sun XL, Hu G (2012) Paeoniflorin protects against ischemia-induced brain damages in rats via inhibiting MAPKs/NF-κB-mediated inflammatory responses. PLoS One 7(11):e49701. doi:10.1371/journal.pone.0049701
23. Dong H, Cui B, Hao X (2019) MicroRNA–22 alleviates inflammation in ischemic stroke via p38 MAPK pathways. Mol Med Rep 20(1):735–744. doi:10.3892/mmr.2019.10269
24. Wang M, Liu Z, Hu S, Duan X, Zhang Y, Peng C, Peng D, Han L (2020) Taohong Siwu Decoction Ameliorates Ischemic Stroke Injury Via Suppressing Pyroptosis. Front Pharmacol 11:590453–590453. doi:10.3389/fphar.2020.590453

25. Chen SF, Pan MX, Tang JC, Cheng J, Zhao D, Zhang Y, Liao HB, Liu R, Zhuang Y, Zhang ZF, Chen J, Lei RX, Li SF, Li HT, Wang ZF, Wan Q (2020) Arginine is neuroprotective through suppressing HIF-1α/LDHA-mediated inflammatory response after cerebral ischemia/reperfusion injury. Mol Brain 13(1):63. doi:10.1186/s13041-020-00601-9
26. Wang L, Lu Y, Guan H, Jiang D, Guan Y, Zhang X, Nakano H, Zhou Y, Zhang Y, Yang L, Li H (2013) Tumor necrosis factor receptor-associated factor 5 is an essential mediator of ischemic brain infarction. J Neurochem 126(3):400–414. doi:10.1111/jnc.12207
27. Wu D, Zhi X, Duan Y, Zhang M, An H, Wei W, Dong K, Zhang Y, Shi J, He X, Zhang J, Wu C, Meng R, Ding Y, Ji X (2019) Inflammatory cytokines are involved in dihydrocapsaicin (DHC) and regional cooling infusion (RCI)-induced neuroprotection in ischemic rat. Brain research 1710:173–180. doi:10.1016/j.brainres.2018.12.033
28. Li F, Geng X, Yip J, Ding Y (2019) Therapeutic Target and Cell-signal Communication of Chlorpromazine and Promethazine in Attenuating Blood–Brain Barrier Disruption after Ischemic Stroke. Cell Transplant 28(2):145–156
29. Geng X, Fu P, Ji X, Peng C, Fredrickson V, Sy C, Meng R, Ling F, Du H, Tan X (2013) Synergetic Neuroprotection of Normobaric Oxygenation and Ethanol in Ischemic Stroke Through Improved Oxidative Mechanism. Stroke 44(5):1418–1425
30. Almekhlafi M, Poli S, Goyal M, Demchuk A (2019) Therapeutic hypothermia in stroke. Quo Vadis? Brain circulation 5(4):157–159. doi:10.4103/bc.bc_62_19
31. Pollmächer T, Haack M, Schuld A, Kraus T, Hinze-Selch D (2000) Effects of antipsychotic drugs on cytokine networks. J Psychiatr Res 34(6):369–382. doi:10.1016/s0022-3956(00)00032-7
32. Basta-Kaim A, Budziszewska B, Jaworska-Feil L, Tetich M, Kubera M, Zajicova A, Holan V, Lasoń W (2004) Effects of lipopolysaccharide and chlorpromazine on glucocorticoid receptor-mediated gene transcription and immunoreactivity: a possible involvement of p38-MAP kinase. European neuropsychopharmacology: the journal of the European College of Neuropsychopharmacology 14(6):521–528. doi:10.1016/j.euroneuro.2004.02.005
33. Masuda K, Kishimoto T (2018) A Potential Therapeutic Target RNA-binding Protein, Arid5a for the Treatment of Inflammatory Disease Associated with Aberrant Cytokine Expression. Curr Pharm Design 24(16):1766–1771. doi:10.2174/1381612824666180426103753
34. Tong Y, Elkin KB, Peng C, Shen J, Li F, Guan L, Ji Y, Wei W, Geng X, Ding Y (2019) Reduced Apoptotic Injury by Phenothiazine in Ischemic Stroke through the NOX-Akt/PKC Pathway. Brain sciences 9 (12). doi:10.3390/brainsci9120378
35. Zeng Z, Zhang Y, Liang X, Wang F, Zhao J, Xu Z, Liu X, Liu X (2019) Qingnao dripping pills mediate immune-inflammatory response and MAPK signaling pathway after acute ischemic stroke in rats. J Pharmacol Sci 139(3):143–150. doi:10.1016/j.jphs.2018.12.009
36. Chen S, Chen H, Du Q, Shen J (2020) Targeting Myeloperoxidase (MPO) Mediated Oxidative Stress and Inflammation for Reducing Brain Ischemia Injury: Potential Application of Natural Compounds. Frontiers in physiology 11:433. doi:10.3389/fphys.2020.00433

37. Barone FC, Hillegass LM, Price WJ, White RF, Lee EV, Feuerstein GZ, Sarau HM, Clark RK, Griswold DE (1991) Polymorphonuclear leukocyte infiltration into cerebral focal ischemic tissue: myeloperoxidase activity assay and histologic verification. J Neurosci Res 29(3):336–345. doi:10.1002/jnr.490290309
38. Cojocaru IM, Cojocaru M, Iliescu I, Botnaru L, Gurban CV, Sfrijan F, Tănăsescu R (2010) Plasma myeloperoxidase levels in patients with acute ischemic stroke. Romanian journal of internal medicine = Revue roumaine de medecine interne 48(1):101–104
39. Rice RA, Pham J, Lee RJ, Najafi AR, West BL, Green KN (2017) Microglial repopulation resolves inflammation and promotes brain recovery after injury. Glia 65(6):931–944. doi:10.1002/glia.23135
40. Fleming JC, Norenberg MD, Ramsay DA, Dekaban GA, Marcillo AE, Saenz AD, Pasquale-Styles M, Dietrich WD, Weaver LC (2006) The cellular inflammatory response in human spinal cords after injury. Brain 129(Pt 12):3249–3269. doi:10.1093/brain/awl296
41. Liu X, Wu Z, Hayashi Y, Nakanishi H (2012) Age-dependent neuroinflammatory responses and deficits in long-term potentiation in the hippocampus during systemic inflammation. Neuroscience 216:133–142. doi:10.1016/j.neuroscience.2012.04.050
42. Duris K, Splichal Z, Jurajda M (2018) The Role of Inflammatory Response in Stroke Associated Programmed Cell Death. Current neuropharmacology 16(9):1365–1374. doi:10.2174/1570159x16666180222155833
43. Hou Y, Wang Y, He Q, Li L, Xie H, Zhao Y, Zhao J (2018) Nrf2 inhibits NLRP3 inflammasome activation through regulating Trx1/TXNIP complex in cerebral ischemia reperfusion injury. Behav Brain Res 336:32–39. doi:10.1016/j.bbr.2017.06.027
44. Tegowski M, Fan C, Baldwin AS (2018) Thioridazine inhibits self-renewal in breast cancer cells via DRD2-dependent STAT3 inhibition, but induces a G(1) arrest independent of DRD2. 293 (41):15977–15990. doi:10.1074/jbc.RA118.003719
45. Tsai C, Ikematsu K, Sakai S, Matsuo A, Nakasono I (2011) Expression of Bcl2l1, Clcf1, IL-28ra and Pias1 in the mouse heart after single and repeated administration of chlorpromazine. Legal medicine (Tokyo Japan) 13(5):221–225. doi:10.1016/j.legalmed.2011.04.006
46. Nicolas CS, Amici M, Bortolotto ZA, Doherty A, Csaba Z, Fafouri A, Dournaud P, Gressens P, Collingridge GL, Peineau S (2013) The role of JAK-STAT signaling within the CNS. Jak-stat 2(1):e22925. doi:10.4161/jkst.22925
47. Li L, Sun L, Qiu Y, Zhu W, Hu K, Mao J (2020) Protective Effect of Stachydrine Against Cerebral Ischemia-Reperfusion Injury by Reducing Inflammation and Apoptosis Through P65 and JAK2/STAT3 Signaling Pathway. Front Pharmacol 11:64–64. doi:10.3389/fphar.2020.00064
48. Sui Y, Bian L, Ai Q, Yao Y, Yu M, Gao H, Zhang A, Fu X, Zhong L, Lu D (2019) Gastrodin Inhibits Inflammasome Through the STAT3 Signal Pathways in TNA2 Astrocytes and Reactive Astrocytes in Experimentally Induced Cerebral Ischemia in Rats. Neuromol Med 21(3):275–286. doi:10.1007/s12017-019-08544-8
49. Liu CC, Huang ZX, Li X, Shen KF, Liu M, Ouyang HD, Zhang SB, Ruan YT, Zhang XL, Wu SL, Xin WJ, Ma C (2018) Upregulation of NLRP3 via STAT3-dependent histone acetylation contributes to painful

neuropathy induced by bortezomib. Exp Neurol 302:104–111. doi:10.1016/j.expneurol.2018.01.011

50. Cheng H, Lv M, Mi R, Xue G (2020) Amifostine ameliorates cerebral ischaemia-reperfusion injury via p38-mediated oxidative stress and mitochondrial dysfunction. Folia neuropathologica 58(4):334–346. doi:10.5114/fn.2020.102436
51. Li D, Ren W, Jiang Z, Zhu L (2018) Regulation of the NLRP3 inflammasome and macrophage pyroptosis by the p38 MAPK signaling pathway in a mouse model of acute lung injury. Mol Med Rep 18(5):4399–4409. doi:10.3892/mmr.2018.9427
52. Bracken CP, Fedele AO, Linke S, Balrak W, Lisy K, Whitelaw ML, Peet DJ (2006) Cell-specific Regulation of Hypoxia-inducible Factor (HIF)-1alpha and HIF-2alpha Stabilization and Transactivation in a Graded Oxygen Environment. J Biol Chem 281(32):22575–22585
53. Talwar H, Bauerfeld C, Bouhamdan M, Farshi P, Liu Y, Samavati L (2017) MKP-1 negatively regulates LPS-mediated IL-1β production through p38 activation and HIF-1α expression. Cell Signal 34:1–10. doi:10.1016/j.cellsig.2017.02.018
54. Jung JE, Lee HG, Cho IH, Chung DH, Yoon SH, Yang YM, Lee JW, Choi S, Park JW, Ye SK, Chung MH (2005) STAT3 is a potential modulator of HIF-1-mediated VEGF expression in human renal carcinoma cells. FASEB journal: official publication of the Federation of American Societies for Experimental Biology 19(10):1296–1298. doi:10.1096/fj.04-3099fje
55. Papadia S, Soriano FX, Léveillé F, Martel MA, Dakin KA, Hansen HH, Kaindl A, Sifringer M, Fowler J, Stefovska V, McKenzie G, Craigon M, Corriveau R, Ghazal P, Horsburgh K, Yankner BA, Wyllie DJ, Ikonomidou C, Hardingham GE (2008) Synaptic NMDA receptor activity boosts intrinsic antioxidant defenses. Nature neuroscience 11(4):476–487. doi:10.1038/nn2071
56. Li Y, Xiang L, Wang C, Song Y, Miao J, Miao M (2021) Protection against acute cerebral ischemia/reperfusion injury by Leonuri Herba Total Alkali via modulation of BDNF-TrKB-PI3K/Akt signaling pathway in rats. Biomedicine pharmacotherapy = Biomedecine pharmacotherapie 133:111021. doi:10.1016/j.biopha.2020.111021
57. Li W, Zhu Q, Xu X, Hu X (2021) MiR-27a-3p suppresses cerebral ischemia-reperfusion injury by targeting FOXO1. Aging 13. doi:10.18632/aging.202866
58. Nyandwi J, Ko Y, Jin H, Yun S, Park S, Kim H (2020) Rosmarinic acid inhibits oxLDL-induced inflammasome activation under high-glucose conditions through downregulating the p38-FOXO1-TXNIP pathway. Biochem Pharmacol 182:114246. doi:10.1016/j.bcp.2020.114246
59. Li X, Kover KL, Heruth DP, Watkins DJ, Moore WV, Jackson K, Zang M, Clements MA, Yan Y (2015) New Insight Into Metformin Action: Regulation of ChREBP and FOXO1 Activities in Endothelial Cells. Molecular endocrinology. (Baltimore Md) 29(8):1184–1194. doi:10.1210/me.2015-1090
60. Zeng R, Luo D, Li H, Zhang Q, Lei S, Chen J (2019) MicroRNA-135b alleviates MPP-mediated Parkinson's disease in in vitro model through suppressing FoxO1-induced NLRP3 inflammasome and pyroptosis. Journal of clinical neuroscience: official journal of the Neurosurgical Society of Australasia 65:125–133. doi:10.1016/j.jocn.2019.04.004

61. Kim D, Kim S, Lee B, Lee E, Chung K, Moon K, An H, Kim K, Yu B, Chung H (2017) Effect of betaine on hepatic insulin resistance through FOXO1-induced NLRP3 inflammasome. J Nutr Biochem 45:104–114. doi:10.1016/j.jnutbio.2017.04.014
62. Kortylewski M, Feld F, Krüger K, Bahrenberg G, Roth R, Joost H, Heinrich P, Behrmann I, Barthel A (2003) Akt modulates STAT3-mediated gene expression through a FKHR (FOXO1a)-dependent mechanism. J Biol Chem 278(7):5242–5249. doi:10.1074/jbc.M205403200
63. Sun W, Wang B, Qu XL, Zheng BQ, Huang WD, Sun ZW, Wang CM, Chen Y (2019) Metabolism of Reactive Oxygen Species in Osteosarcoma and Potential Treatment Applications. Cells 9 (1). doi:10.3390/cells9010087
64. Raeis V, Philip-Couderc P, Roatti A, Habre W, Sierra J, Kalangos A, Beghetti M, Baertschi AJ (2010) Central venous hypoxemia is a determinant of human atrial ATP-sensitive potassium channel expression: evidence for a novel hypoxia-inducible factor 1alpha-Forkhead box class O signaling pathway. Hypertension (Dallas, Tex: 1979) 55 (5):1186–1192. doi:10.1161/hypertensionaha.109.148767

Figures

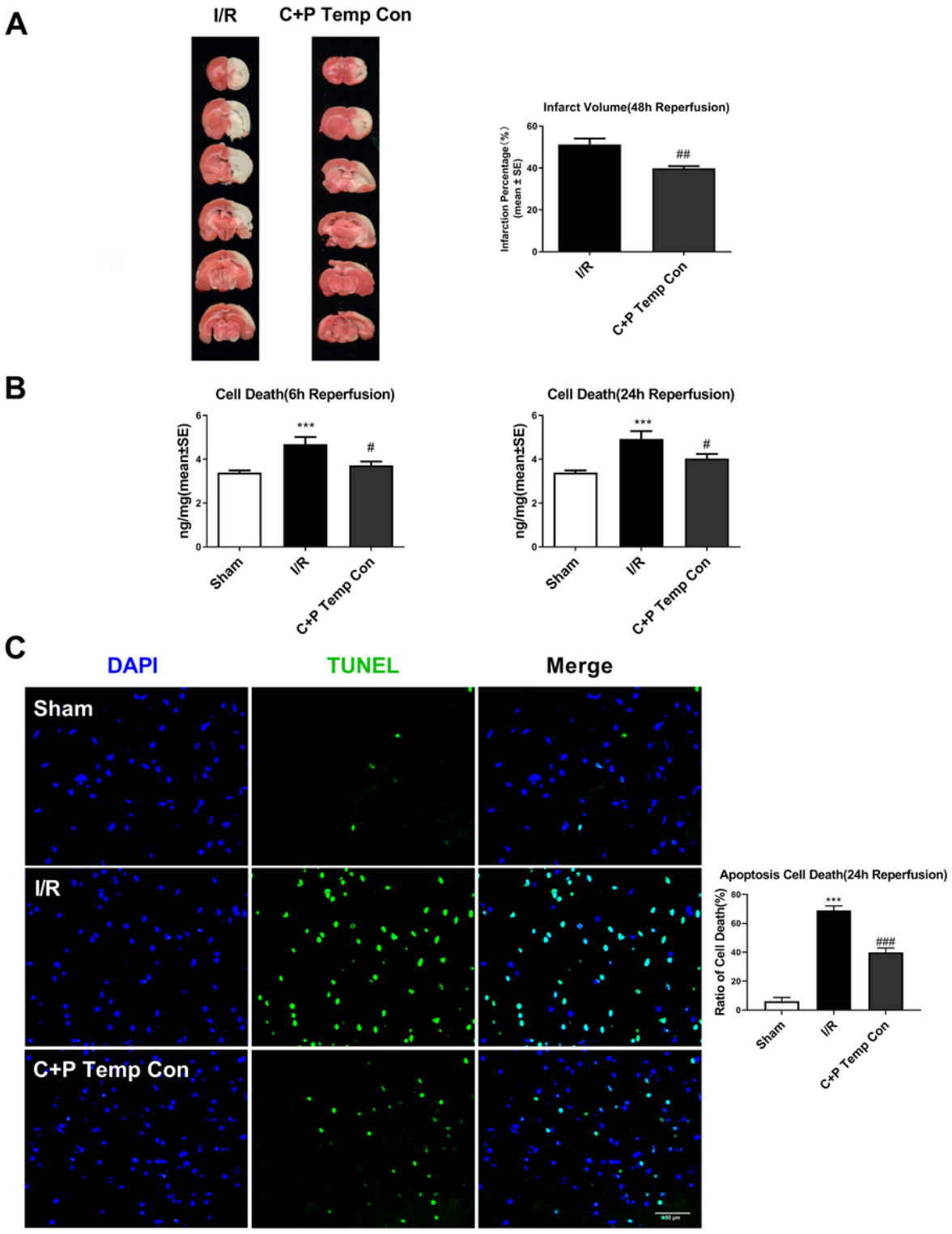

Figure 1

C+P attenuated neural injury under ischemic conditions. (A) TTC staining illustrates infarct volumes in MCAO rats with or without C+P at 48 h reperfusion. Compared to the I/R group, C+P significantly decreased neural damage at 48 h reperfusion (n=7). (B) Cell death as measured by ELISA significantly increased at 6 and 24 h reperfusion. There was a significant decrease with C+P at 6 and 24 h reperfusion (n=7). (C)Apoptotic cell death was markedly greater at 24 h reperfusion but significantly diminished by

C+P at 24 hours reperfusion as detected by the TUNEL assay (n=7). Scale bar = 50 μm. ***p < 0.001, as compared to the sham group; #p < 0.05, ##p < 0.01, and ###p < 0.001, as compared to the I/R group. The data are presented as the mean ± SE.

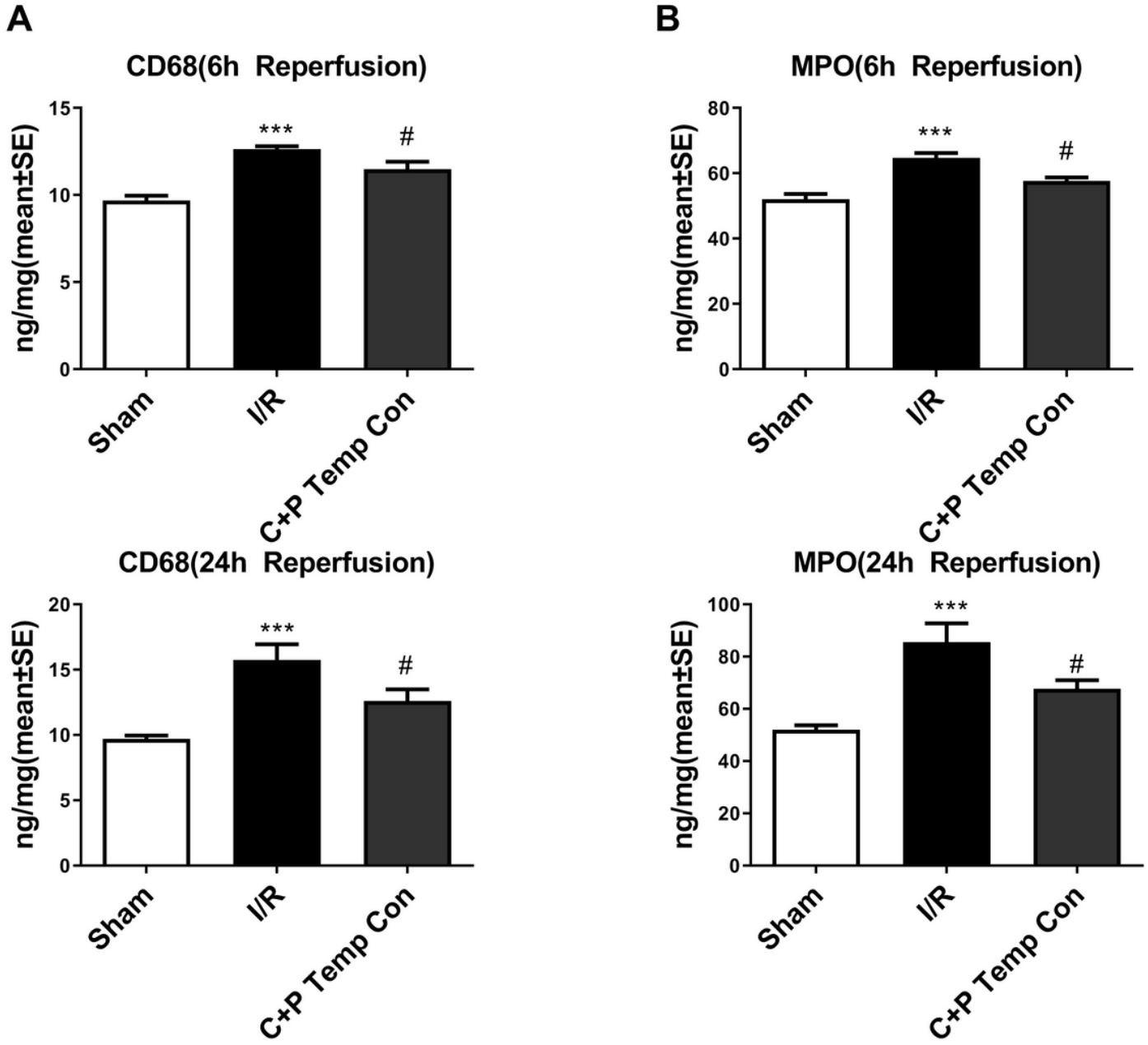

Figure 2

C+P reduced CD68 and MPO levels in ischemic brain tissue. Quantitative analysis of (A) CD68 and (B) MPO levels as measured by ELISA in ischemic brain tissue. Decreased levels of CD68 and MPO were observed with C+P and temperature control at 6 and 24 h reperfusion (n = 7). ***p < 0.001, as compared to the sham group; #p < 0.05, as compared to the I/R group. The data are presented as the mean ± SE.

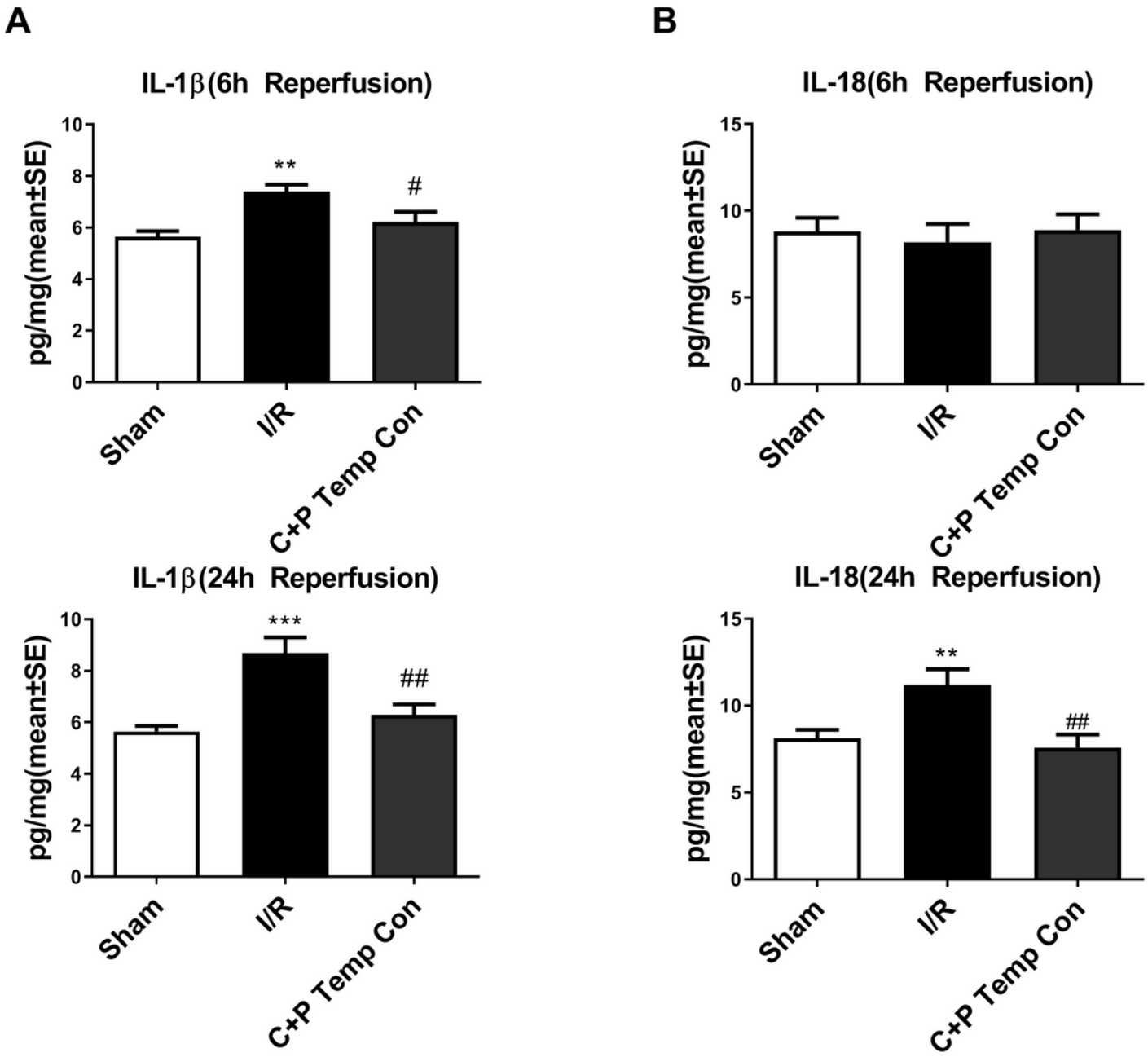

Figure 3

C+P decreased IL-1β and IL-18 levels after stroke. Quantitative analysis of (A) IL-1β and (B) IL-18 levels as measured by ELISA in ischemic brain tissue. C+P significantly attenuated the elevation of IL-1β at 6 and 24 h reperfusion, as well as IL-18 at 24 h reperfusion (n = 7). **p < 0.01 and ***p < 0.001, as compared to the sham group; #p < 0.05 and ##p < 0.01, as compared to the I/R group. The data are presented as the mean ± SE.

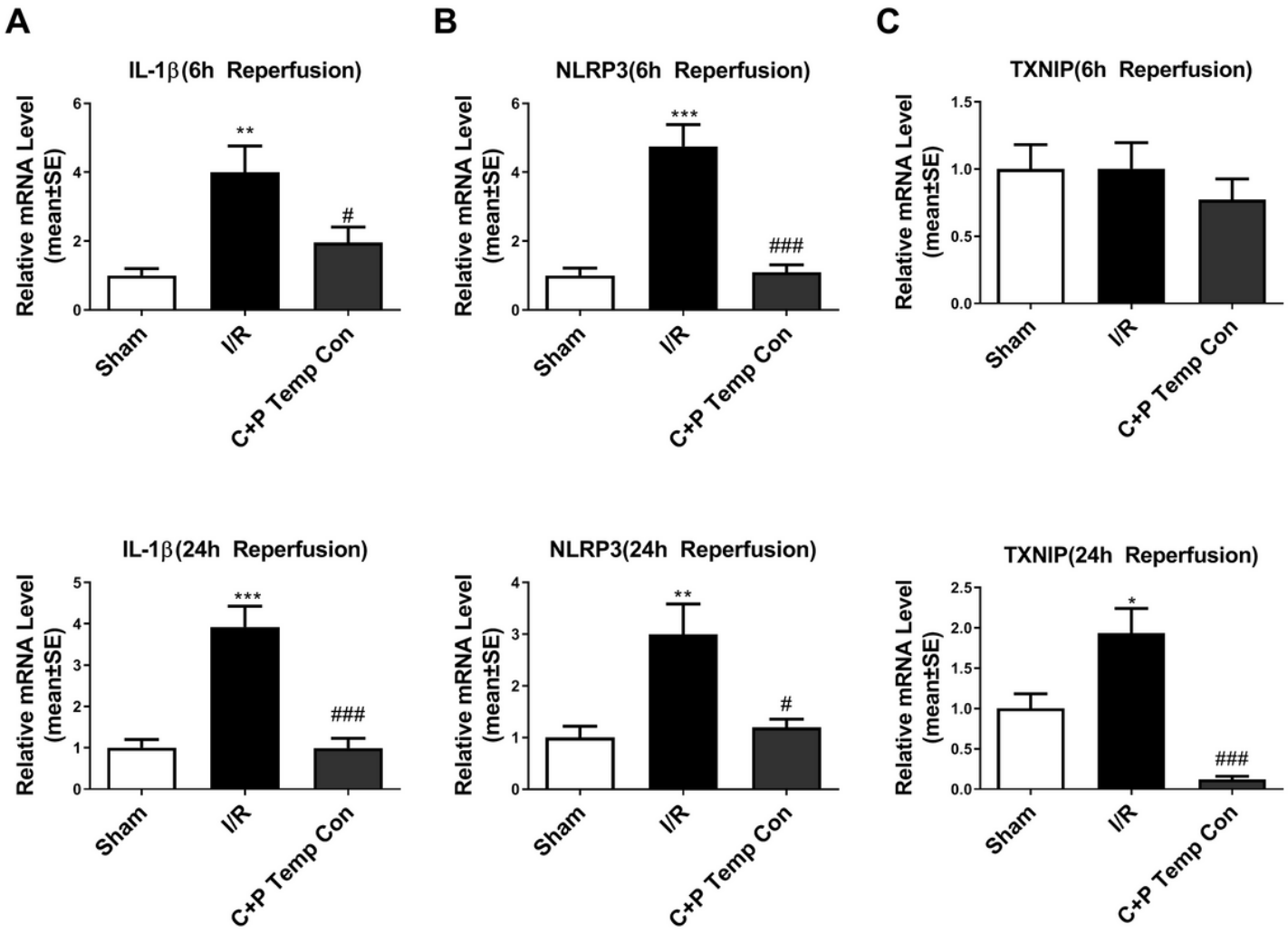

Figure 4

C+P suppressed IL-1β, NLRP3, and TXNIP mRNA levels after stroke. (A) IL-1β, (B) NLRP3, and (C) TXNIP as evaluated by quantitative real-time PCR at 6 h and 24 h reperfusion. The mRNA levels of IL-1β, NLRP3, and TXNIP increased after I/R, but were reduced with C+P at 6 and 24 h reperfusion, with the exclusion of TXNIP at 6 h reperfusion (n = 7). *p < 0.05, **p < 0.01, ***p < 0.001, as compared to the sham group; #p < 0.05 and ###p < 0.001, as compared to the I/R group. The data are presented as the mean ± SE.

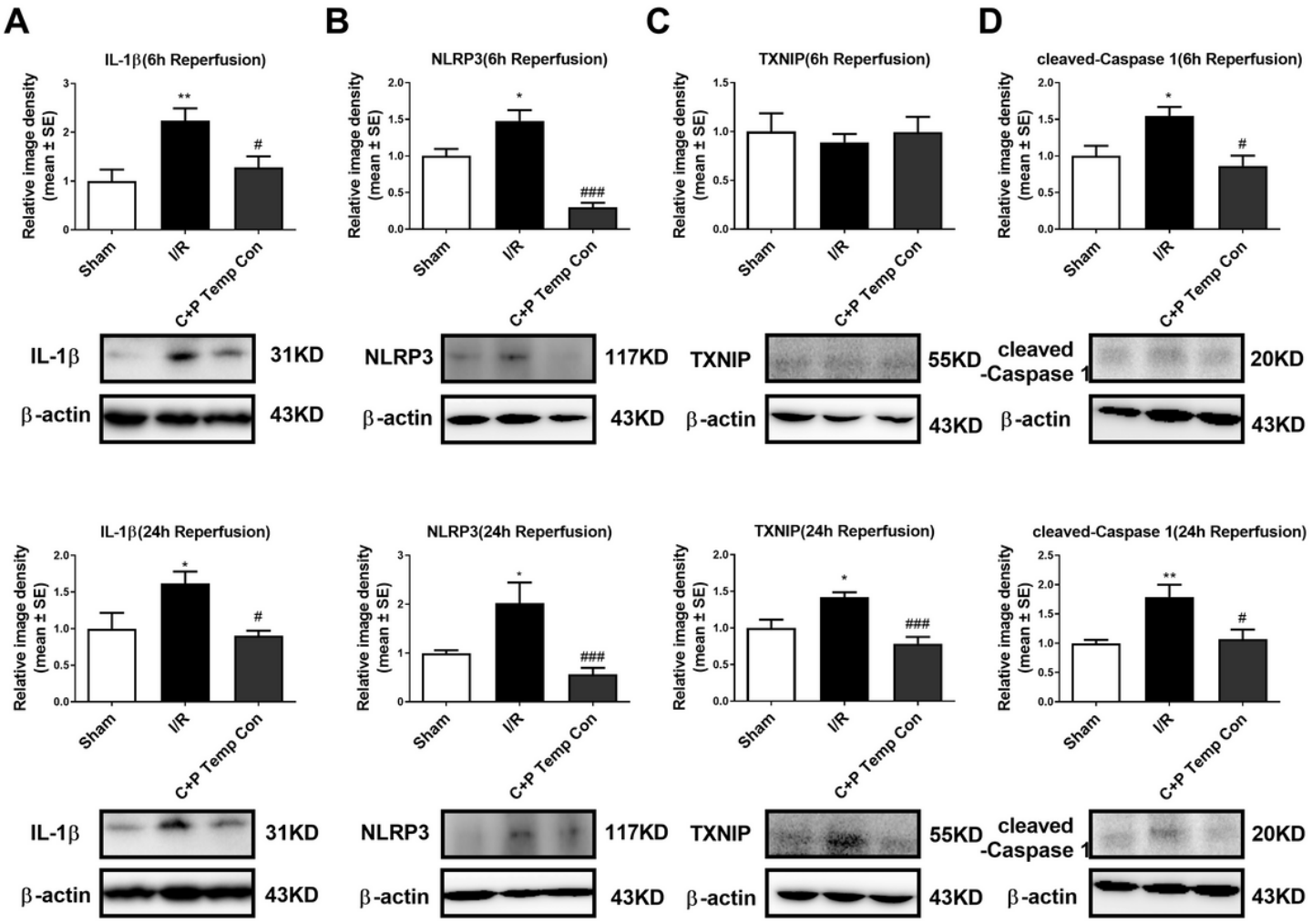

Figure 5

C+P suppressed IL-1β, NLRP3, TXNIP and cleaved-Caspase 1 expressions after ischemia/reperfusion. (A) IL-1β, (B) NLRP3, (C) TXNIP, and (D) cleaved-Caspase 1 as evaluated by Western blot at 6 h and 24 h reperfusion. The protein levels of IL-1β, NLRP3, TXNIP, and cleaved-Caspase 1 increased after I/R, but reduced with C+P at 6 and 24 h reperfusion, with the exception of TXNIP at 6 h reperfusion (n = 7). *p < 0.05 and **p < 0.01, as compared to the sham group; #p < 0.05 and ###p < 0.001, as compared to the I/R group. The data are presented as the mean ± SE. The representative immunoblots are presented.

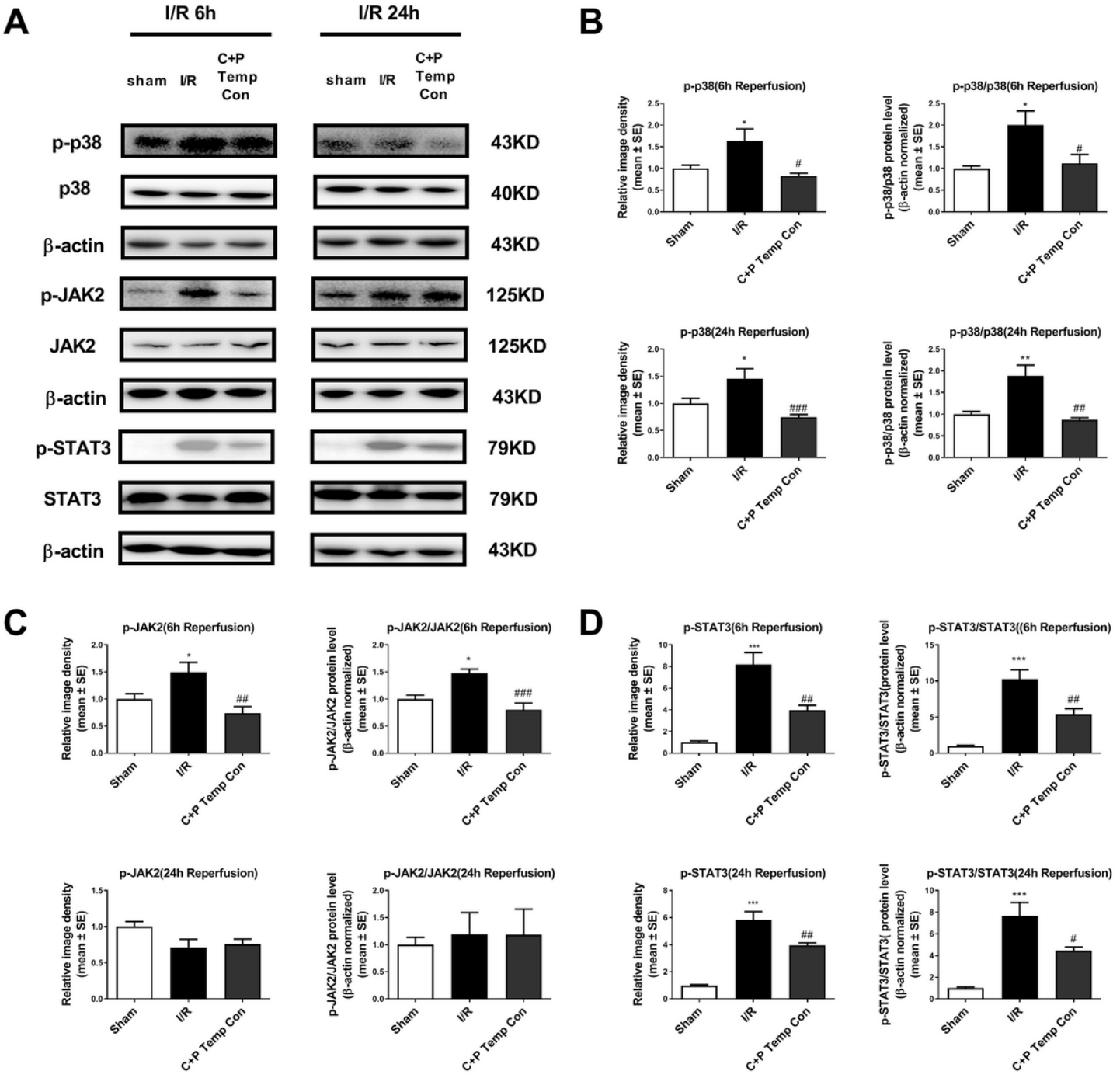

Figure 6

C+P decreased expressions of JAK2/STAT3 and p38 pathways induced by cerebral ischemia. (A) Representative bands of phosphorylated and total protein expressions of p38, JAK2, and STAT3 as detected by Western blot assay at 6 and 24 h reperfusion. β-actin protein was used as an internal control. Bar graphs show semiquantitative levels of (B) p-p38 and p-p38/p38; (C) p-JAK2 and p-JAK2/JAK2; and (D) p-STAT3 and p-STAT3/STAT3 as determined by band density analysis. MCAO significantly increased phosphorylation levels of p38 and STAT3 at 6 h and 24 h reperfusion, as well as JAK2 at 6 h reperfusion. C+P treatment decreased the phosphorylation of p38 and JAK2/STAT3 as compared with stroke group (n

= 7). *p < 0.05, **p < 0.01, and ***p < 0.001, as compared to the sham group; #p < 0.05, ##p < 0.01, and ###p < 0.001, as compared to the I/R group. The data are presented as the mean ± SE.

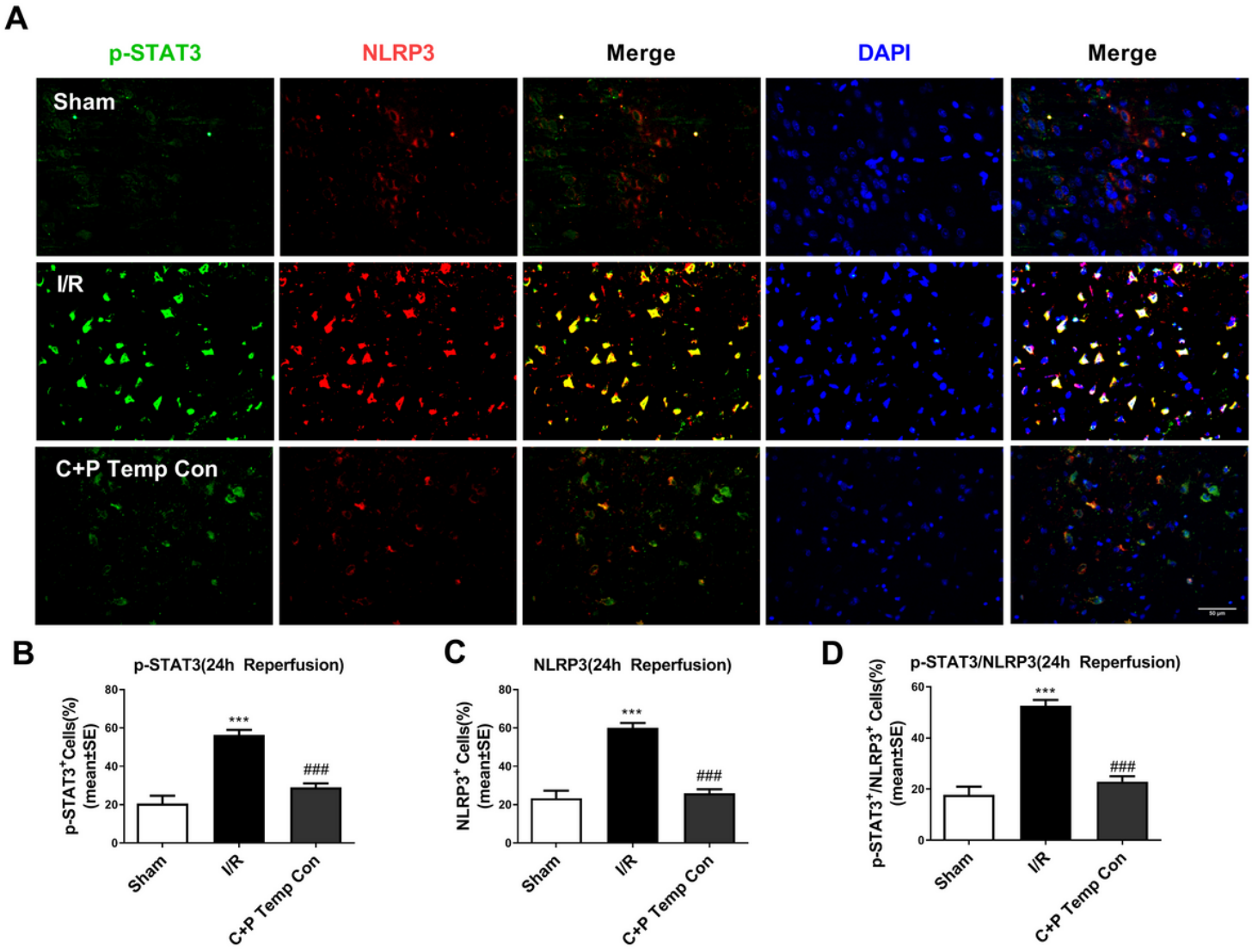

Figure 7

Co-localization of p-STAT3 and NLRP3. (A) Representative images of NLRP3 (red) and p-STAT3-positive cells (green) in sham, I/R, and C+P groups with temperature regulation at 24h reperfusion. Cellular nuclei are visible as blue DAPI stains. Quantitative assessment of (B) p-STAT3 and (C) NLRP3 positive cells in the rat brain. (D) Quantitative assessment of p-STAT3/NLRP3 double positive cells in the rat brain. C+P repressed the expressions of p-STAT3 and NLRP3, and the co-localization of p-STAT3 and NLRP3 at 24 h reperfusion after stroke. (n=6) ***p < 0.001, as compared to the sham group; ###p < 0.001, as compared to the I/R group. The data are presented as the mean ± SE. Scale bar = 50 μm.

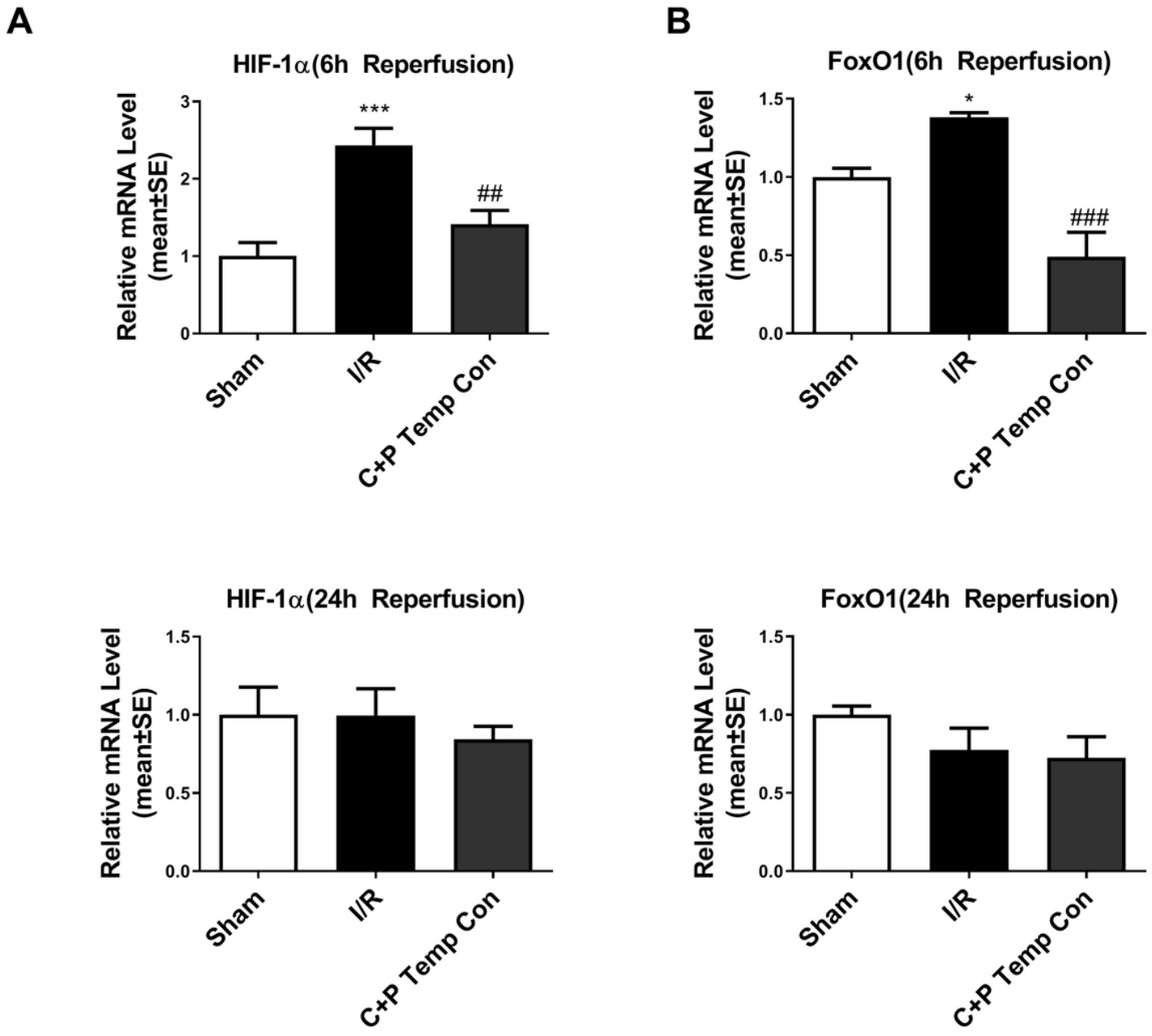

Figure 8

C+P suppressed HIF-1α and FoxO1 mRNA levels after stroke. (A) HIF-1α and (B) FoxO1 were evaluated by quantitative real-time PCR at 6 h and 24 h reperfusion. The mRNA levels of HIF-1α and FoxO1 increased after I/R, but C+P reduced the quantities of HIF-1α and FoxO1 at 6 h reperfusion(n = 7). *p < 0.05 and ***p < 0.001, as compared to the sham group; ##p < 0.01 and ###p < 0.001, as compared to the I/R group. The data are presented as the mean ± SE.

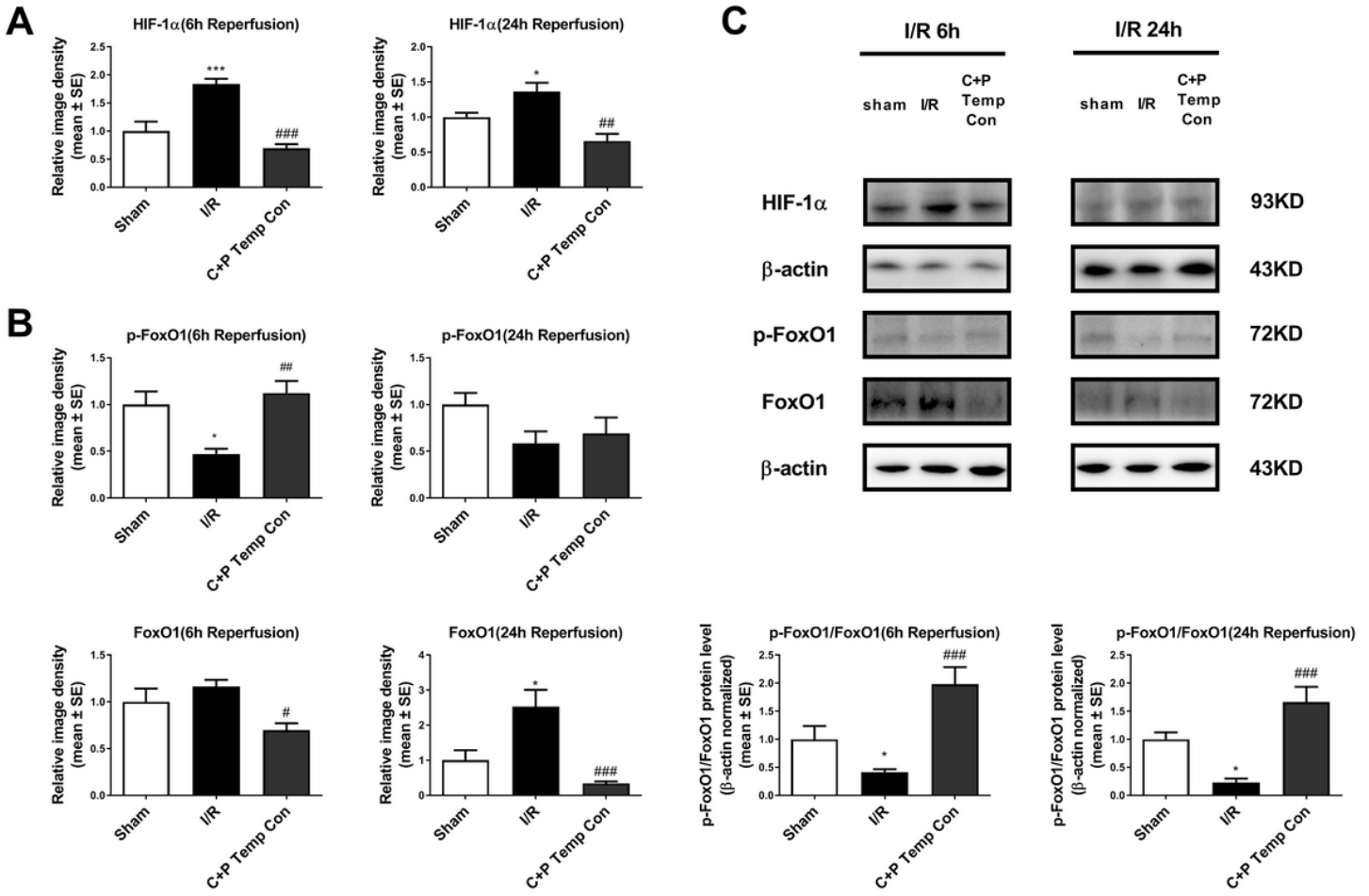

Figure 9

C+P suppressed the activation of HIF-1α and FoxO1 induced by cerebral ischemia. (A) Bar graphs show semiquantitative levels of HIF-1α as determined by band density analysis. (B) Bar graphs show semiquantitative levels of p-FoxO1, FoxO1, and p- FoxO1/ FoxO1 as determined by band density analysis. (C) Representative bands of HIF-1α, p-FoxO1, and FoxO1 as detected by Western blot assay at 6 and 24 h reperfusion. β-actin protein was used as an internal control. In addition, C+P reduced the elevated expression of HIF-1α after stroke at 6 and 24h reperfusion. MCAO significantly decreased the phosphorylation level of FoxO1 while C+P attenuated this trend at 6 h reperfusion. Moreover, the expression of FoxO1 increased at 24 h reperfusion, while C+P reduced its levels at 6 and 24 h reperfusion. The ratio of p-FoxO1/FoxO1 significantly decreased after MCAO, but increased with C+P at 6 and 24 h reperfusion (n = 7). *p < 0.05 and ***p < 0.001, as compared to the sham group; #p < 0.05, ##p < 0.01, and ###p < 0.001, as compared to the I/R group. The data are presented as the mean ± SE.

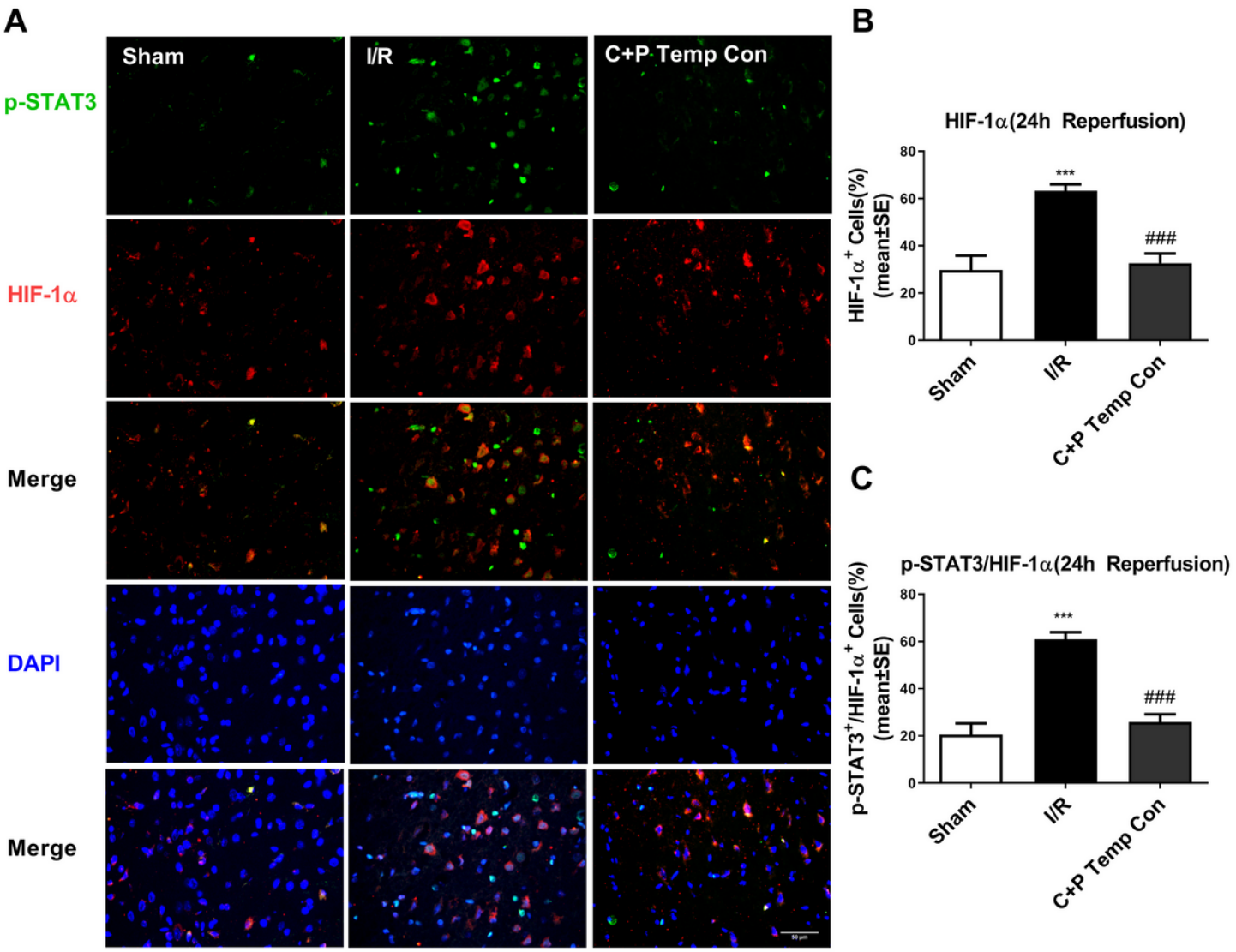

Figure 10

The Co-localization of p-STAT3 and HIF-1α. (A) Representative images of HIF-1α (red) and p-STAT3-positive cells (green) in sham, I/R, and C+P, with temperature regulation at 24h reperfusion. Cellular nuclei are visible as blue DAPI stains. (B) Quantitative assessment of HIF-1α positive cells in the rat brain. (C) Quantitative assessment of p-STAT3/ HIF-1α double positive cells in the rat brain. C+P suppressed the expression of HIF-1α and co-localization of p-STAT3 and HIF-1α at 24 h reperfusion after stroke. (n=6) ***p < 0.001, as compared to the sham group; ###p < 0.001, as compared to the I/R group. The data are presented as the mean ± SE. Scale bar = 50 μm.

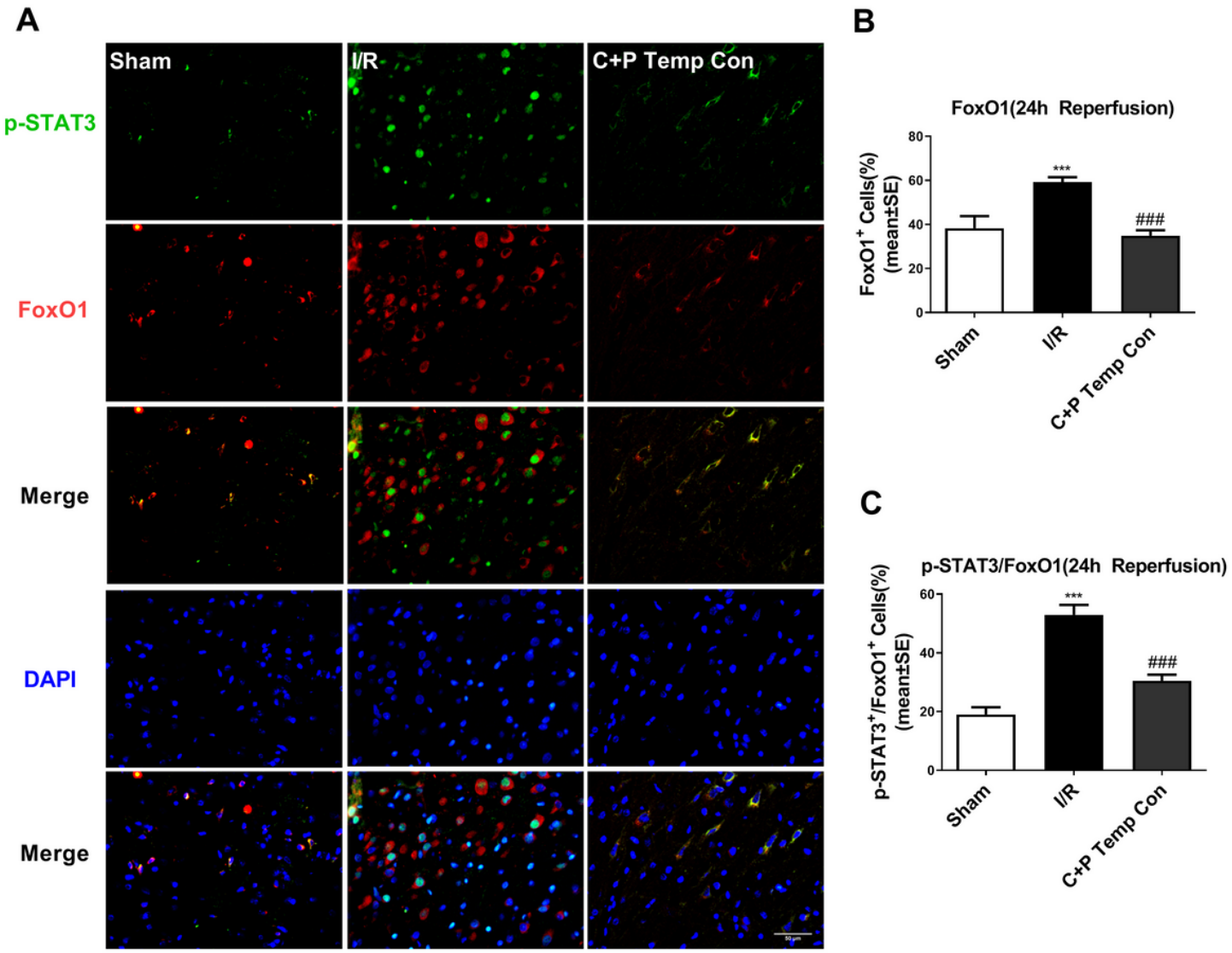

Figure 11

The Co-localization of p-STAT3 and FoxO1. (A) Representative images of FoxO1 (red) and p-STAT3-positive cells (green) in sham, I/R, and C+P with temperature regulation at 24h of reperfusion. Cellular nuclei are visible as blue DAPI stains. (B) Quantitative assessment of FoxO1 positive cells. (C) Quantitative assessment of p-STAT3/ FoxO1 double positive cells. C+P suppressed the expression of FoxO1 and co-localization of p-STAT3 and FoxO1 at 24 h reperfusion after stroke. (n=6) ***p < 0.001, as compared to the sham group; ###p < 0.001, as compared to the I/R group. The data are presented as the mean ± SE. Scale bar = 50 μm.